Electronic Supplementary Material (ESI) for Chemical Science.
This journal is © The Royal Society of Chemistry 2014
CREATED USING THE RSC LaTeX PCCP ARTICLE TEMPLATE – SEE www.rsc.org/electronicfiles FOR DETAILS

Electronic Supplementary Information for: Resolving Molecular Orbitals Self-decoupled from Semiconductor Surfaces

Jing Hui He, Wei Mao, Wei Chen, Kai Wu, Han Song Cheng, and Guo Qin Xu*

Contents

1 Pixel analysis of tip state transition

Figure S1 shows the STM tip changed its state from Normal(I)→Blured(II)→Tadpole-like(III)→dummbell-like(IV). The IV state was the same state as in the Figure 1b in the main text, except for its tracing-up scanning direction. This also proves that the orientation of dumbbell features is independent of scanning directions.

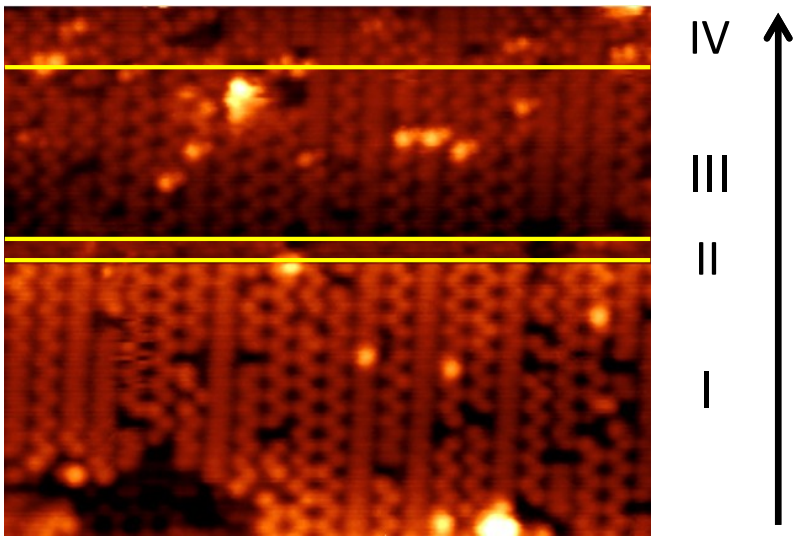

Supplementary Figure 1 Evolution of the STM tip state from normal to orbital resolution during tracing-up STM scanning. Zone I-V show four different tip states. I: normal; II: blurred; III: Tadpole-like state, the left halves of the dumbbells are brighter that the right parts; IV: another submolecular state (as same as in Figure 1b of the main text), the right halves of these dumbbells are bright than the left parts. Scanning condition: I=200 pA, V= -1.6 V.

In STM experiments, both the geometric and electronic structures of the tip and sample contribute to the tunneling conductance. Given the same sample and scanning conditions (the same scanning area, scanning

direction, tunneling bias and current), the improvement of resolution can only be attributed to the change of the STM tip. We carefully searched the scanning area for the points where the resolution was transiting from normal to submolecular (or vice versa, Figure S1) by analyzing the STM images pixel by pixel (Figure S2) in consecutive scanning right before and after the submolecular state. In Figure S2c, **A** and **B** marked the locations where the tip state was changing, corresponding to the state transitions: I→II and II→III in Figure S1, respectively. In Figure S2e, point **C** was located due to the out-of-phase splitting of two neighboring scanning lines at this point, as shown in Figure S2f. This pixel is assigned for the transition from III to IV. When STM scanned back to those point in next frame, Figures Figure S2b and Figure S2d showed there was neither extra defects produced, nor external atoms or molecule falling on. Thus, we propose that the submolecular resolution should only be induced via modification of the tip apex by external molecules coming from dosing source.

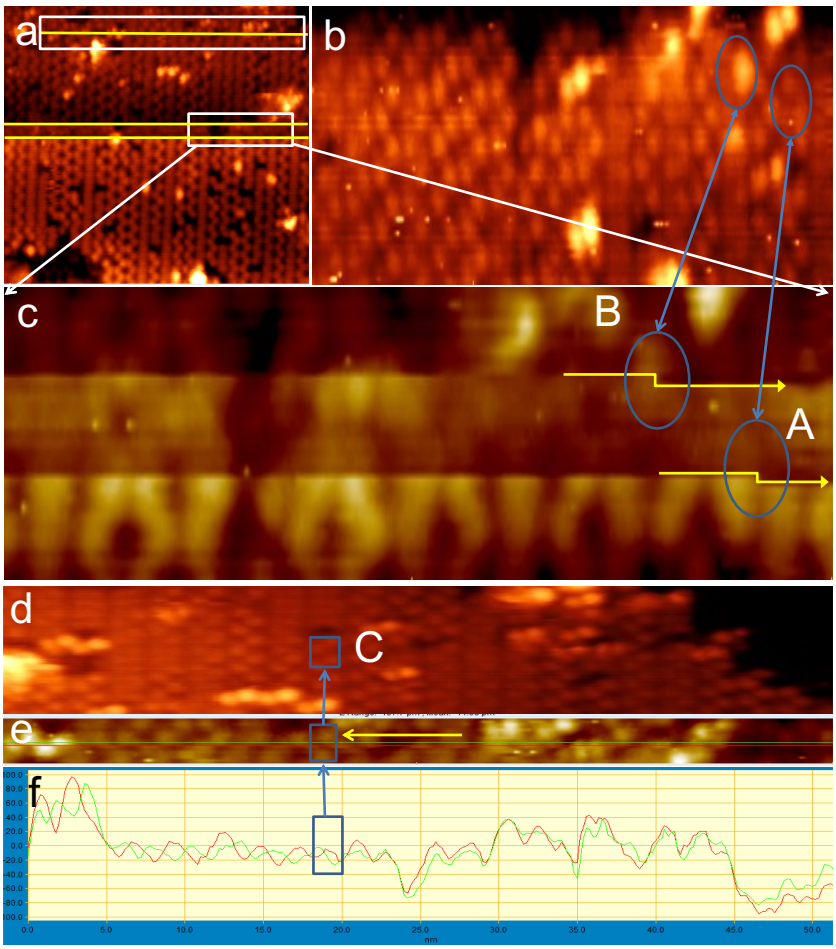

Supplementary Figure 2 Pixel analysis of the STM images where the STM tip was changing its state. (a) STM image from Figure S1. The rectangles marked the area for pixel analysis. (b) The tracing-down scanning of the area in Figure S2c after the tip converted to submolecular resolution in the previous tracing up scanning. (c) The zoomed-in image of the area marked in Figure S2a. "A" and "B" refer to the tip state-changing points. The arrows indicate the scanning directions. (d) Tracing-down image of the area marked by the longer rectangle in Figure S2a after the tip converted to the submolecular resolution. (e) The zoomed-in image of the area marked by the longer rectangle in Figure S2a. The green and red scanning lines is before and on the tip changing point **C**, respectively. The arrow indicates the scanning direction. (f) Profiles of two adjacent lines in Figure S2e for the tip state changing from state III to IV. Scanning condition: I=200 pA, V= -1.6 V.

2 Rotational barriers of N-C bonds in nitrosobenzene adducts

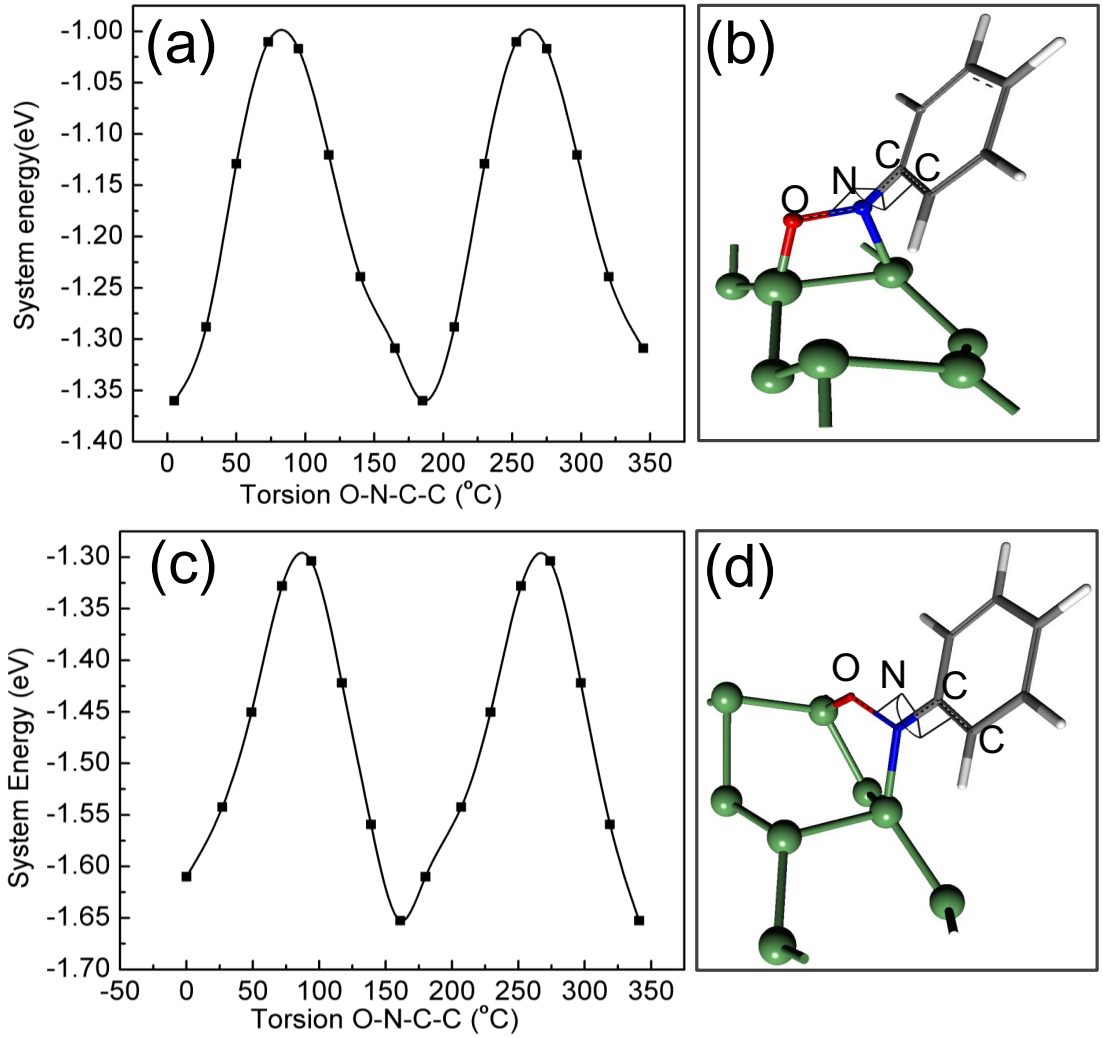

Supplementary Figure 3 Energy variations of the phenyl rings rotating along C-N bond in the two nitrosoadducts. (a)interdimer adduct and (b) its definition of O-N-C-C torsion angle. (c)intradimer adduct and (d) its definition of O-N-C-C torsion angle.

3 Molecular orbitals of free benzene

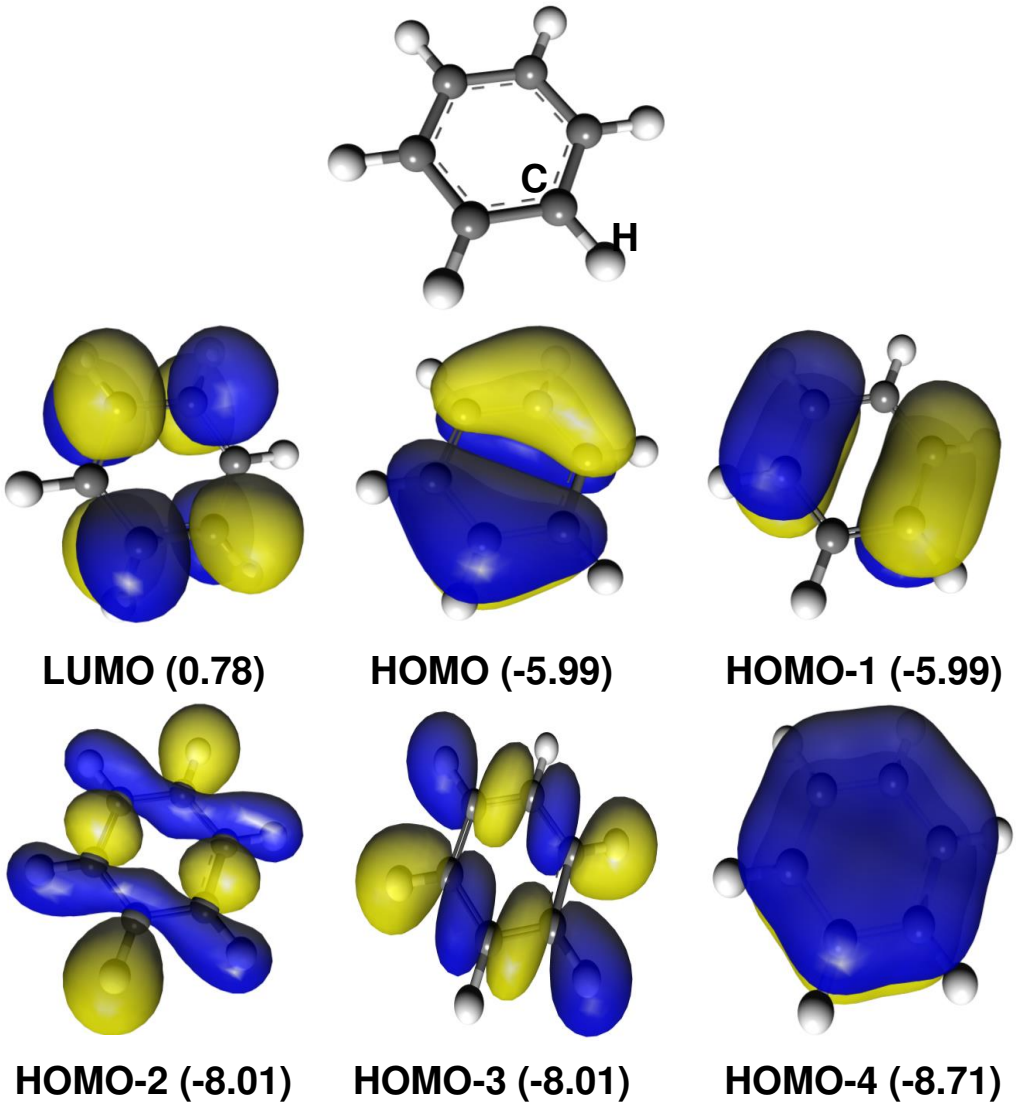

Supplementary Figure 4 Molecular orbitals of benzene. The energies in parentheses refer to the vacuum level as zero. The LUMO are delocalized π^* orbitals HOMO and HOMO-1 are two degenerate π orbitals. HOMO-2 and HOMO-3 belongs to two degenerate σ orbitals. HOMO-3 is the lowest π orbital. The isovalue to plot the orbitals is 0.03 e/Å^3. Blue and yellow indicate different phases of wave functions.

4 Cartesian coordinates of the two nitrosoadducts

The structure models are periodic slabs, therefore their structures are listed in .xtl format. They can be read by many model software such as VESTA. To use the file, copy the data between two rules of the table and paste them into a text file, which should be saved with the name xxx.xtl.

Supplementary Table 1 .xtl file format of the interdimer nitrosoadduct.

TITLE	interdimer	nitrosoadduct			
CELL					
16.34726	8.173629	22.71584	90	90	90
SYMMETRY	NUMBER	1			
SYMMETRY	LABEL	P1			
ATOMS					
NAME	X	Y	Z		
H	0.37004	0.66255	0.33206		
H	0.31877	0.51807	0.42191		
H	0.45338	0.86087	0.53109		
H	0.50180	0.00674	0.44180		
H	0.46006	0.90906	0.34145		
C	0.38780	0.70676	0.37586		
C	0.35888	0.62471	0.42578		
C	0.38110	0.68259	0.48227		
C	0.43385	0.81976	0.48729		
C	0.46130	0.90051	0.43705		
C	0.43839	0.84502	0.38087		
N	0.35331	0.61302	0.53485		
O	0.30668	0.47021	0.52938		
Ge	0.12795	0.02777	0.65024		
Ge	0.12500	0.00000	0.91147		
Ge	0.12500	1.00000	0.91147		
Ge	0.36866	0.49271	0.66891		
Ge	0.37500	0.50000	0.91147		
Ge	0.12846	0.48022	0.65575		
Ge	0.12500	0.50000	0.91147		
Ge	0.37583	0.02150	0.63957		
Ge	0.37500	0.00000	0.91147		
Ge	0.37500	1.00000	0.91147		
Ge	0.00015	0.74790	0.77918		
Ge	0.24891	0.22509	0.78531		
Ge	0.00023	0.24539	0.77972		
Ge	0.25037	0.75260	0.78413		
Ge	0.17442	0.75183	0.61708		
Ge	0.12500	0.75000	0.84580		
Ge	0.30602	0.30558	0.59393		
Ge	0.37500	0.25000	0.84580		
Ge	0.99963	0.99751	0.71264		
Ge	0.24419	0.48876	0.73018		
Ge	0.99733	0.49624	0.71442		
Ge	0.25650	0.98797	0.71243		
Ge	0.14953	0.26078	0.57561		
Ge	0.12500	0.25000	0.84580		
Ge	0.33226	0.73545	0.60866		
Ge	0.37500	0.75000	0.84580		
Ge	0.63038	0.97802	0.65213		
Ge	0.62500	0.00000	0.91147		
Ge	0.62500	1.00000	0.91147		
Ge	0.87030	0.47712	0.65146		
Ge	0.87500	0.50000	0.91147		
Ge	0.62798	0.51158	0.65048		
Ge	0.62500	0.50000	0.91147		
Ge	0.87048	0.01306	0.65184		
Ge	0.87500	0.00000	0.91147		
Ge	0.87500	1.00000	0.91147		
Ge	0.49987	0.74961	0.77963		
Ge	0.75053	0.24768	0.78465		
Ge	0.50082	0.23628	0.77977		
Ge	0.74910	0.74546	0.78464		
Ge	0.66383	0.74685	0.57895		
Ge	0.62500	0.75000	0.84580		
Ge	0.83637	0.24520	0.57852		
Ge	0.87500	0.25000	0.84580		
Ge	0.49870	0.99550	0.70981		
Ge	0.74871	0.49732	0.72109		
Ge	0.50478	0.49263	0.71784		
Ge	0.75079	0.99703	0.72265		
Ge	0.68807	0.24506	0.61667		
Ge	0.62500	0.25000	0.84580		
Ge	0.81255	0.74496	0.61675		
Ge	0.87500	0.75000	0.84580		
EOF					

Supplementary Table 2 .xtl file format of the intradimer nitrosoadduct.

TITLE	intradimer	nitrosoadduct			
CELL					
16.34726	8.173629	22.71584	90	90	90
SYMMETRY	NUMBER	1			
SYMMETRY	LABEL	P1			
ATOMS					
NAME	X	Y	Z		
H	0.44734	0.14757	0.42706		
H	0.38866	0.00600	0.51461		
H	0.24950	0.68617	0.39998		
H	0.30963	0.82643	0.31238		
H	0.40847	0.05756	0.32533		
C	0.40517	0.04451	0.42075		
C	0.37245	0.96537	0.47007		
C	0.31589	0.83615	0.46335		
C	0.29272	0.78736	0.40580		
C	0.32665	0.86640	0.35688		
C	0.38275	0.99539	0.36392		
N	0.28593	0.75344	0.51382		
O	0.19792	0.74129	0.51487		
Ge	0.12848	0.01996	0.64793		
Ge	0.12500	0.00000	0.91147		
Ge	0.12500	1.00000	0.91147		
Ge	0.37444	0.50615	0.64825		
Ge	0.37500	0.50000	0.91147		
Ge	0.12813	0.47909	0.64835		
Ge	0.12500	0.50000	0.91147		
Ge	0.37383	0.00929	0.65132		
Ge	0.37500	0.00000	0.91147		
Ge	0.37500	1.00000	0.91147		
Ge	-0.00001	0.75018	0.77819		
Ge	0.99999	0.75018	0.77819		
Ge	0.24933	0.25192	0.78271		
Ge	0.00033	0.25039	0.77900		
Ge	0.25022	0.75063	0.78264		
Ge	0.16766	0.74670	0.59837		
Ge	0.12500	0.75000	0.84580		
Ge	0.30646	0.25665	0.60864		
Ge	0.37500	0.25000	0.84580		
Ge	0.00061	0.00041	0.71119		
Ge	0.24986	0.50106	0.71788		
Ge	0.00023	0.49924	0.71151		
Ge	0.24875	0.00180	0.71902		
Ge	0.15705	0.25008	0.57361		
Ge	0.12500	0.25000	0.84580		
Ge	0.31955	0.76067	0.59773		
Ge	0.37500	0.75000	0.84580		
Ge	0.63024	0.98281	0.64964		
Ge	0.62500	0.00000	0.91147		
Ge	0.62500	1.00000	0.91147		
Ge	0.87114	0.48083	0.65055		
Ge	0.87500	0.50000	0.91147		
Ge	0.63047	0.51826	0.64944		
Ge	0.62500	0.50000	0.91147		
Ge	0.87124	0.01693	0.65042		
Ge	0.87500	0.00000	0.91147		
Ge	0.87500	1.00000	0.91147		
Ge	0.49982	0.75052	0.77876		
Ge	0.75081	0.24980	0.78425		
Ge	0.49965	0.25182	0.77913		
Ge	0.74914	0.75075	0.78433		
Ge	0.66451	0.75079	0.57666		
Ge	0.62500	0.75000	0.84580		
Ge	0.83723	0.24897	0.57734		
Ge	0.87500	0.25000	0.84580		
Ge	0.50292	0.00255	0.71271		
Ge	0.75029	0.50034	0.72084		
Ge	0.50259	0.50068	0.71194		
Ge	0.75036	0.00007	0.72071		
Ge	0.68858	0.25037	0.61485		
Ge	0.62500	0.25000	0.84580		
Ge	0.81305	0.74877	0.61524		
Ge	0.87500	0.75000	0.84580		
EOF					